Physical origin of in-plane lattice spacing oscillations measured by reflection high-energy electron diffraction during epitaxial growth

J. D. Fuhr[1] and P. Müller[2]

[1]*Centro Atómico Bariloche, CNEA, and CONICET, Av. E. Bustillo 9500, R8402AGP, Bariloche, Argentina*

[2]*CINaM-CNRS, UPR 3118, Aix-Marseille Université, Campus de Luminy, Case 913, F-13288 Marseille Cedex, France*

(Received 12 July 2011; revised manuscript received 8 September 2011; published 7 November 2011)

Intensity oscillations of the specular (0,0) RHEED spot during layer-by-layer growth are well known, whereas the associated oscillation of the position of the RHEED streaks remains more controversial. We revisit the problem of the origin of the peak-to-peak oscillations observed in RHEED spectra during layer-by-layer epitaxial growth. For this purpose we perform solid-on-solid KMC simulations to describe the growth, and we use the kinematical approximation to simulate RHEED intensity profiles. We show that the peak-to-peak oscillations result from the angular dispersion of the incident beam and the periodic oscillation of the size of the growing islands, without the need of invoking the strain relaxation in the islands.

DOI: 10.1103/PhysRevB.84.195429 PACS number(s): 61.05.jh, 81.15.Aa, 68.35.Gy

I. INTRODUCTION

Since the work of Royer,[1] the regular oriented overgrowth of a crystalline material onto a single crystal surface is called epitaxy. Thermodynamics considerations allow us to classify three different modes of epitaxial growth:[2] a 2D layer-by-layer mode,[3] a 3D mode,[4] and a mixed mode.[5] The 2D layer-by-layer mode is essential for producing high-quality electronic devices by molecular beam epitaxy.[6] Depending on the vicinality of the exposed surface, 2D growth may occur by step flow or by 2D nucleation,[7] also known as Frank van der Merwe (FvM) mode. In the FvM mode, 2D islands nucleate and then spread to form a complete monolayer on which a new 2D nucleation process takes place, leading to the layer-by-layer growth.[3]

Reflection high-energy electron diffraction (RHEED) is an in-situ technique that enables us to monitor the FvM growth, since the intensity of the specular (0,0) RHEED spot exhibits extremely regular oscillations whose period exactly corresponds to the growth rate of a single monolayer.[8,9] A simple interpretation was given in Refs. 10 and 11: Reflectivity maxima characterize the scattering by a smooth surface (without 2D islands), while reflectivity minima correspond to scattering by the most rough surface when the island density is maximum (close to half coverage).

A decade ago, Massies and co-workers[12] discovered that in $In_xGa_{1-x}/GaAs$, the peak-to-peak distance between two diffracted (0,1) and (0,−1) RHEED streaks also oscillates with the growth rate period. This effect was, later on, observed for a large number of other heteroepitaxial systems.[13–25] The origin of these oscillations was attributed to the lattice mismatch between the substrate and the deposited film:[12] At complete coverage (and in the absence of any plastic relaxation) the in-plane lattice parameter of the epitaxial film is imposed by its underlying substrate (homogeneous deformation of the epilayers), while at incomplete coverage the 2D islands elastically relax by their edges. It follows that the in-plane lattice of the surface layer oscillates with the growth rate period, between an extremum (when the island density is maximum) and a nominal value (for the pseudomorphous surface layer). It was thus astonishing to find peak-to-peak oscillations in homo-epitaxial growth, that means in the absence of any lattice mismatch,[23,26,27] contradicting the explanation given in Ref. 12. A first explanation, still based on Ref. 12, was given in Refs. 28–30, where it was shown that at the nanoscale, one can define a so-called active misfit even in homoepitaxy. However, the amplitude of the so-calculated peak-to-peak oscillations are one order of magnitude smaller than those reported in many experiments. It was the case for V for which the oscillation was later-on attributed to a surface reconstruction induced by oxygen incorporation,[19,30,31] but it is also the case for other systems as the one reported in Fig. 1. Moreover, in perfect epitaxy, without any plastic relaxation, the constraint imposed by the substrate leads to a vanishing mean deformation averaged over all the surface, even in heteroepitaxial systems.

In this paper, we revisit the problem of the origin of these peak-to-peak oscillations. For this purpose, we simulate the RHEED pattern evolution during FvM growth. Our main result is that the peak-to-peak oscillations originate from the angular dispersion of the incident beam and the width broadening of the truncated rods. In other words, it is not necessary to invoke the strain relaxation in the islands to retrieve the peak-to-peak oscillations with the growth rate period. As a consequence, the amplitude of the oscillations is found to depend upon the angle dispersion at work.

II. MODEL

A complete calculation of RHEED intensities needs to use the dynamical theory of electron scattering. However, it is well known that for a quantitative analysis of the position of the Bragg streaks, a simple kinematical approach is sufficient. In this approximation, the incident and diffracted beams, with wave vectors $\vec{k}_i$ and $\vec{k}_f$ respectively, are represented by the amplitudes[32]

$$A_{\text{in}} = A_i e^{i\vec{k}_i\cdot\vec{r}} \tag{1}$$

$$A_{\text{out}} = A_i \left[\sum_n f_n(\vec{s}) e^{i\vec{s}\cdot\vec{r}_n}\right] e^{i\vec{k}_f\cdot\vec{r}}, \tag{2}$$

where $f_n(\vec{s})$ is the atomic scattering factor for the nth atom located at position $\vec{r}_n$, and $\vec{s} = \vec{k}_f - \vec{k}_i$ is the momentum

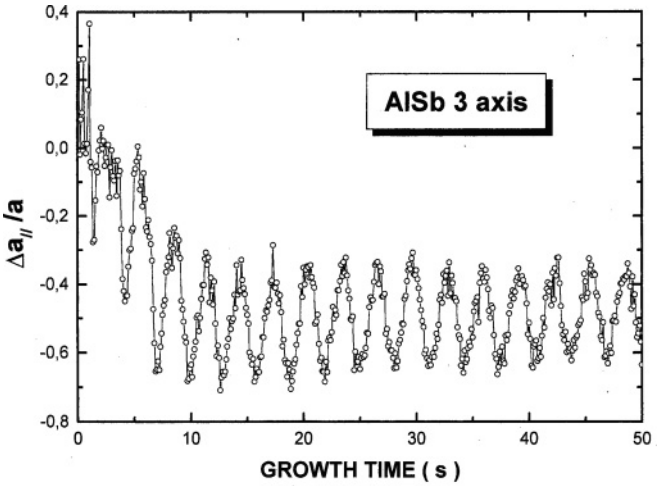

FIG. 1. In-plane lattice oscillations deduced from the position of the RHEED streaks recorded during homoepitaxial recorded growth at $T = 500^\circ$ C of AlSb (growth rate: 0.35 ML/sec). Courtesy of J.Massies, CRHEA, Sophia-Antipolis.

transfer. As we are considering elastic scattering, the incident and scattered wave vectors are related to the constant energy by

$$E = \frac{\hbar^2}{2m_e}|\vec{k}_i|^2 = \frac{\hbar^2}{2m_e}|\vec{k}_f|^2. \tag{3}$$

In principle, the sum in Eq. (2) should run over all atoms in the system. However, the inelastic effects represented by a mean free path for the electrons means that deeper layers of the surface contribute less to the scattered wave amplitude A_{out}. We introduce this effect by dividing the system atoms in layers and adding a factor β_i for each layer i, with $\beta_0 = 1$ the factor for the outmost surface layer and $\beta_{i+1} \leqslant \beta_i$. We therefore rewrite Eq. (2) as

$$A_{\text{out}} = A_i \left[\sum_i \beta_i \left(\sum_{n\in i} f_n(\vec{s}) e^{i\vec{s}\cdot\vec{r}_n} \right) \right] e^{i\vec{k}_f\cdot\vec{r}}. \tag{4}$$

When the surface is not flat, the height of each layer i will depend on the lateral position. The RHEED intensity I will then be proportional to $|A_{\text{out}}|^2/|A_{\text{in}}|^2$, i.e.,

$$I \propto \left| \sum_i \beta_i \left(\sum_{n\in i} f_n(\vec{k}_f - \vec{k}_i) e^{i(\vec{k}_f-\vec{k}_i)\cdot\vec{r}_n} \right) \right|^2. \tag{5}$$

In a real experiment, the incident electron beam diverges and the electrons in the beam have a range of energies. This is reflected in a dispersion in the incident wave vector $\vec{k}_i$. We introduce this effect by calculating a mean value over $\vec{k}_i$

$$\overline{I} \propto \int d^3k_i \, g(\vec{k}_i) \left| \sum_i \beta_i \left(\sum_{n\in i} f_n(\vec{k}_f - \vec{k}_i) e^{i(\vec{k}_f-\vec{k}_i)\cdot\vec{r}_n} \right) \right|^2, \tag{6}$$

where $g(\vec{k}_i)$ gives the dispersion reflecting the experimental conditions.

In the following, we take $\beta_0 = 1$ and $\beta_{i\neq 0} = 0$, valid for ideal RHEED calculations. We also neglect all dependence of the atomic scattering factor f_n on the momentum transfer.

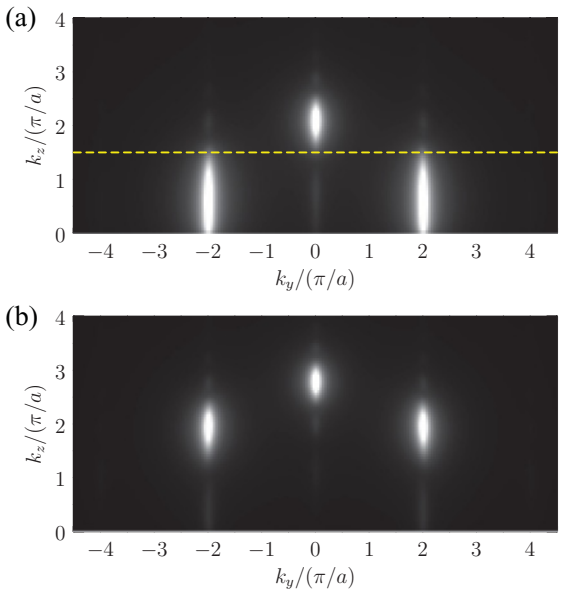

FIG. 2. (Color online) Simulated RHEED intensity patterns for different incident angles: (a) $\alpha_i = 1.5^\circ$ and (b) $\alpha_i = 2.0^\circ$.

III. RESULTS

To calculate the integral in Eq. (6), we used Monte Carlo integration[33] with a dispersion relation chosen as

$$g(\vec{k}_i) = A \frac{a_\parallel^2}{a_\parallel^2 + (k - \overline{k}_i)^2} \frac{a_\perp^2}{a_\perp^2 + (k_\perp)^2}, \tag{7}$$

where $k = |\vec{k}_i|$ is the total wave vector with mean value $\overline{k}_i$, $k_\perp$ is the perpendicular component of $\vec{k}_i$ with respect to the mean incident direction given by α_i, A is a normalization factor, and the parameters $a_\parallel$ and $a_\perp$ represent incident energy and angular dispersions, respectively. For the Monte Carlo integration, we use a sampling composed of the order of 10^5 incident wave vectors. For simulating RHEED patterns (Fig. 2), we also take into account the detector precision by taking a mean value of the intensity obtained with Eq. (6), weighted by a Lorentzian centered in each value of the scattered wave vector $\vec{k}_f$.

The parameters needed for the calculations are then: the incident wave vector $k_i = |\vec{k}_i|$, the incident angle α_i, the dispersion parameters $a_\parallel$ and $a_\perp$, and the crystal structure of the surface, which defines the distance between layers and the lateral positions of the atoms in each layer.

Typical electron energies E in RHEED experiments are around 30 keV, which corresponds to an incident wave vector of $k_i \simeq 70$ Å^{-1}. We can define k_i for each system in terms of $2\pi/a$, a being the surface lattice parameter. For example, in Cu(100), with $a_{Cu} = 3.61$ Å, we have $k_i \simeq 40 \times 2\pi/a_{Cu}$. The energy dispersion is $\Delta E/E \simeq 10^{-4}$, which corresponds to an incident wave vector dispersion of $\Delta k_i/k_i \simeq 5 \times 10^{-5}$. Finally, the incident angle α_i is around 1°, with a divergence of around 0.01°. Notice that dispersions $10^{-5} < \Delta k/k < 10^{-3}$ and $10^{-3} < \Delta\alpha/\alpha < 10^{-1}$ roughly correspond to $0.01/a < a_\parallel, a_\perp < 0.2/a$.

A. Simulated RHEED patterns for clean surface

We first study the dependence of the spectra with the incident angle. In Fig. 2, we show the simulated spectra for a flat surface, with $k_i = 40 \times 2\pi/a$, $a_\parallel = a_\perp = 0.1/a$, and two incident angles: $\alpha_i = 1.5^\circ$ and $\alpha_i = 2.0^\circ$. The bright spots at $k_{f,y} = 0$ correspond to the condition of constructive interference $k_{f,x} = k_{i,x}$, resulting in an angle for the scattered electrons equal to the incident angle α_i. Other spots should appear for the other conditions of constructive interference $k_{f,x} = k_{i,x} - 2\pi n/a$, but they correspond to much higher $k_{f,z}$. For large enough α_i, we can see the appearance of satellite spots with the condition $k_{f,y} = \pm 2\pi/a$, and the normal wave vector component satisfying $k_{f,z} = \sqrt{k_{i,z}^2 - k_{f,y}^2}$. The incident energy dispersion is reflected in the elongated shape of the spots in the k_z direction. The RHEED intensity profile is then obtained along a straight line as shown in Fig. 2(a).

To study the effect of the incident energy and angle dispersions, we performed calculations for fixed incident angle $\alpha_i = 1.5^\circ$, and different values of dispersion parameters $a_\parallel$ and $a_\perp$. The obtained profiles are shown in Fig. 3, where we see that the main effect is a lateral enlargement of the spots which depends on the angular dispersion parameter $a_\perp$. We also see in this figure that the peak is asymmetric, and its maximum is shifted toward lower values of k_y when $a_\perp$ is increased.

B. Simulated RHEED intensity during epitaxial growth

We simulated the 2D crystal growth by solid-on-solid kinetic Monte Carlo (KMC) simulations.[34] We used a square grid composed of 600×600 unit cells, where each point in the grid is characterized by the height of the top atom occupying the corresponding lateral position. All atoms on the surface have the possibility to move to the top of a neighbor site, with a probability given by its corresponding energy barrier. In this way, we can simulate multilayer growth with the only constraint being that no bulk vacancies can be formed within this model. The jump rate of an atom to a neighbor site is given by $\nu = \nu_0 \exp^{-E_b/k_B T}$, with ν_0 a prefactor which was taken constant and equal to 10^{13} sec^{-1}. E_b is an energy barrier calculated as $E_b = E_d + n\,E_n$, with E_d the diffusion barrier of an isolated atom on top of a flat surface, n the number of first neighbors at the same level, and E_n the bonding energy to these first neighbor atoms. As we are not trying to simulate any specific system, the parameters of the model were chosen in order to have a layer-by-layer growth mode, with islands of reasonable size. We took a diffusion barrier of $E_d = 0.6$ eV and a bonding energy with neighbors in the same layer of $E_n = 0.3$ eV. To simulate the growth, we considered a constant flux of incident atoms on the surface equal to one monolayer per second (1 ML/sec).

For each islands configuration during growth, we calculate a RHEED intensity profile along a straight line as shown in Fig. 2(a). As in the experiments, the intensity profiles are then fitted by a function of the form

$$f(k_y) = \sum_{i=1}^{3} \frac{A_i}{a_i^2 + (k_y - k_i)^2} \tag{8}$$

to determine the position of the maximum k_i.

Figure 4(a) shows several intensity profiles calculated for increasing coverages $0 < \theta < 1$. We can see a reduction of the intensity with increased coverage up to 0.5 ML. Moreover, the peak asymmetry leads to a shift of the maximum position. Figure 4(b) shows the calculated peak displacement, obtained by fitting with Eq. (8), for increasing coverages $0 < \theta < 2$, and for different values of the dispersion parameters $a_\parallel$, $a_\perp$. The peak displacement exhibits an oscillating behavior with a period of 1 ML, and the main effect comes from the angular dispersion characterized by $a_\perp$: The weaker the dispersion, the smaller the oscillating behavior. Therefore, for a perfect instrument there should be no oscillations. We believe that this is the fundamental reason for which peak-to-peak oscillations have only been reported in RHEED experiments but not in

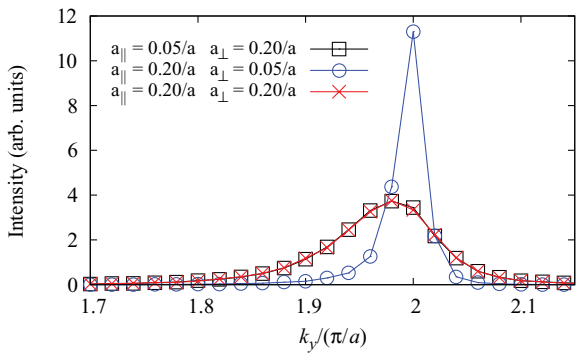

FIG. 3. (Color online) Simulated RHEED intensity profiles along the line shown in Fig. 2(a), for different incident energy and angle dispersions.

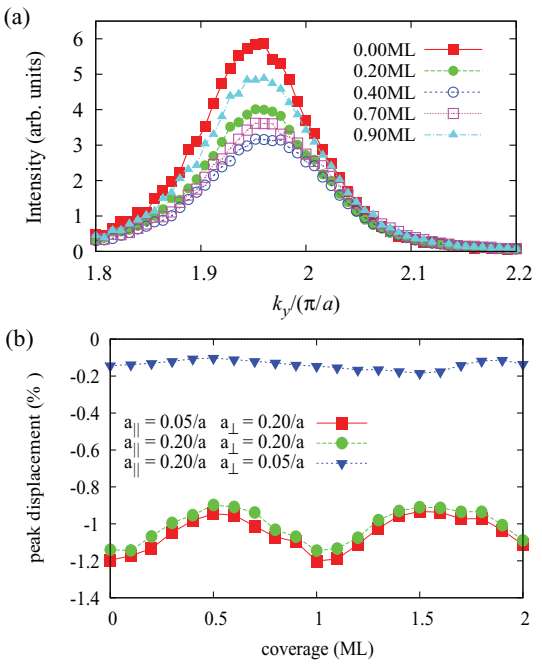

FIG. 4. (Color online) (a) Intensity RHEED profiles calculated for increasing coverages $0 < \theta < 1$, corresponding to a growth temperature of 550 K. The used dispersion parameters for the RHEED calculations are $a_\parallel = a_\perp = 0.2/a$. (b) Calculated peak displacement vs surface coverage for different values of the dispersion parameters $a_\parallel$ and $a_\perp$.

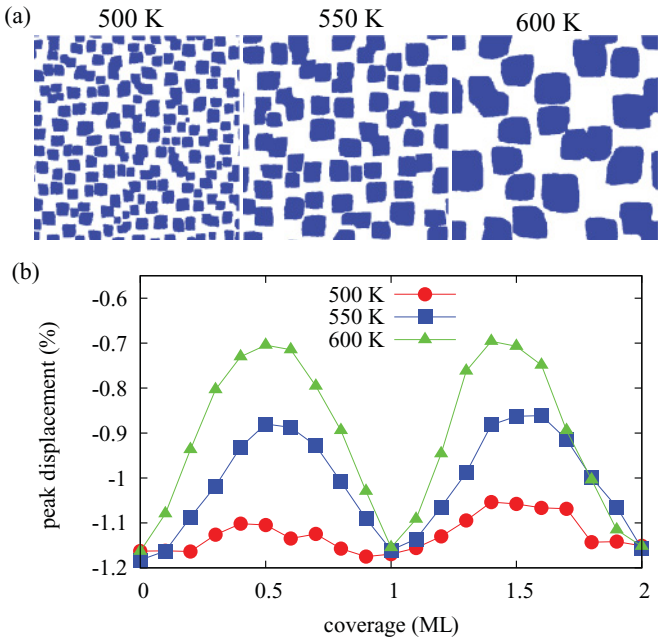

FIG. 5. (Color online) (a) Snapshots of the KMC at 0.5 ML for increasing growth temperatures: 500 K (left panel), 550 K (middle panel), and 600 K (right panel), corresponding to decreasing island densities. (b) Calculated peak displacement vs surface coverage for the three growth conditions.

x-ray diffraction measurements, for which energy and angular dispersions are close to zero compared to RHEED apparatus.

In order to study the effect of island density on the amplitude of the peak displacement oscillations, we perform KMC simulations with increasing growth temperatures (500 K, 550 K, and 600 K) corresponding to decreasing island densities. In Fig. 5(a), we present snapshots corresponding to a deposition of 0.5 ML at each growth temperature, showing that higher growth temperature leads to a lower island density. In Fig. 5(b), we show the calculated peak displacement versus surface coverage. We see that within this island density range the maximum peak displacement remains almost the same, but a higher island density leads to a decrease of the oscillation amplitude. This result can be compared with the temperature variation of the in-plane oscillations reported for several systems (Fe/Fe, V/V, and Nb/Nb) in Ref. 27. In these studied systems, in particular for V/V(001) and Nb/Nb(001) and in the low temperature range, the oscillation amplitude seems to increase with temperature, as it does in our calculations. However, in experiments, for higher temperatures the oscillation amplitude decreases again to attain almost no oscillations at the highest temperatures. For these high temperatures, the island density is lower than what can be reasonably described with the 600 × 600 grid we have used for the KMC simulations.

C. Nature of the oscillations

In Fig. 6, we illustrate the origin of the oscillations on the basis of two main ingredients: (i) the angular dispersion of the incident beam and (ii) the variable width of the truncated rods characteristic of the growing islands. A typical 2D pattern of truncated rods (perpendicular to the figure) is plotted for

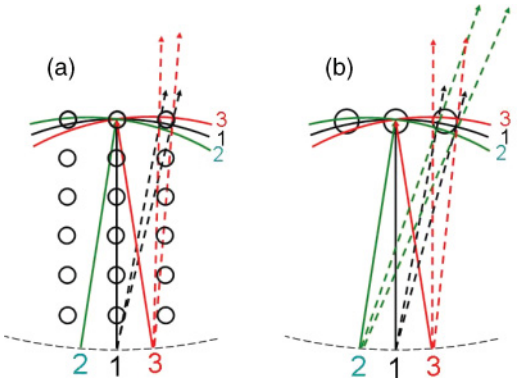

FIG. 6. (Color online) Illustration of the origin of the peak-to-peak oscillations. In both figures are drawn the reciprocal pattern (on the left several truncated rods, on the right only a few relevant rods are drawn), three incident rays, and their associated diffracted beams resulting from the intersection of the corresponding Ewald Sphere with a truncated rod. Incident beams and their corresponding Ewald spheres are respectively labeled 1, 2, and 3.

narrow [Fig. 6(a)] and large [Fig. 6(b)] rods (the smaller the islands, the larger the rod). The tracks of three incident beams are drawn: One (labeled 1) is perfectly oriented in the [01] direction, whereas the two others (labeled 2 and 3) are symmetrically disoriented by an angle $\pm\alpha$. A part of their associated Ewald Spheres (with the same labels 1–3) are also drawn. Let us consider the diffracted conditions of a specific rod. In Fig. 6(a), Ewald construction shows that beam 2 does not contribute to the diffraction (no intersection between the rod and the Ewald Sphere 2), whereas beams 1 and 3 diffract in slightly different directions. It follows that, for a given rod width, the position of the spot diffracted by a [01] beam slightly depends on its angular dispersion value. Furthermore, for a given angular dispersion, the peak position also depends on the rod width as illustrated in Fig. 6(b). Due to the larger rod width, the three beams 1, 2, and 3 fulfill the diffraction conditions so that the position of the diffracted spot cannot coincide with the position obtained from Fig. 6(a), where only the 1 and 3 beams participate to the diffracted beam.

This oversimplified sketch illustrates how the oscillation of the position of the diffracted beam depends on the periodic oscillations of the rod width associated to the 2D island birth and growth, but only in the presence of an angular dispersion of the incident beam.

IV. CONCLUSIONS

Since the first experimental evidence, it has been considered that peak-to-peak oscillations recorded by RHEED during crystal growth have an elastic origin and can be attributed to the lattice mismatch between the substrate and the deposited film, even for homoepitaxy where a so-called active misfit can be defined.[28] However, the fact that in perfect epitaxy the mean deformation averaged over all the surface should be zero even in heteroepitaxial systems calls for a different explanation of the oscillations.

In this paper, we have revisited the origin of these peak-to-peak oscillations in RHEED spectra during layer-by-layer epitaxial growth. Using solid-on-solid KMC simulations to

describe the growth, and the kinematical approximation to simulate RHEED intensity profiles, we have been able to describe the peak-to-peak oscillations without invoking any strain relaxation in the islands. We have shown that these oscillations originate from the angular dispersion characteristic of RHEED instruments that relaxes exact diffraction conditions, and thus allows us to measure a shift of the diffracted peaks as a function of the 2D islands size that varies during the crystal growth. We believe that this is the fundamental reason for which peak-to-peak oscillations during crystal growth have only been reported in RHEED experiments and not in x-ray diffraction measurements, for which energy and angular dispersions are close to zero compared to RHEED apparatus. We have also studied how the growth conditions affect the oscillating behavior. We found that within the density range we can simulate in our grid; while the maximum peak displacement does not depend on the growth conditions, a higher island density leads to a decrease of the oscillation amplitude. This is in agreement with the temperature variation of the in-plane oscillations reported for several systems (Fe/Fe, V/V, and Nb/Nb)[27] in the low temperature range.

ACKNOWLEDGMENTS

J. Massies, A. Saul, R. Kern, and S. Andrieu are acknowledged for fruitful discussions. This work has been done thanks to a PICS Grant No. 4843.

[1] L. Royer, Bull. Soc. Fr. Min. Crist. **51**, 7 (1928).
[2] Bauer, Z. Kristallogr. **110**, 372 (1958).
[3] F. Frank and J. V. der Merwe, Proc. R. Soc. A **198**, 205 (1949).
[4] M. Volmer and A. Weber, Z. Phys. Chem. **119**, 277 (1926).
[5] J. Stranski and L. Krastanov, Ber. Akad. Wiss. Wien **146**, 797 (1938).
[6] R. Kern, G. Le-Lay, and J. J. Métois, in *Current topics in Materials Science*, edited by E. Kaldis (North Holland Publishing Company, Amsterdam, New York, Oxford, 1979), Chap. 3, pp. 132–421.
[7] W. Burton, N. Cabrera, and F. Frank, Philos. Trans. R. Soc. London **243**, 299 (1951).
[8] W. Braun, in *Tracts in Modern Physics*, Vol. 154 (Springer Tracts, Berlin, 1999), p. 216.
[9] A. Ichimiya and P. Cohen, *Reflection High Energy Electron Diffraction* (Cambridge University, Cambridge, 2004).
[10] J. H. Neave, B. A. Joyce, P. J. Dobson, and N. Norton, Appl. Phys. A **31**, 1 (1983).
[11] B. Joyce, P. Dobson, and J. Neave, Surf. Sci. **178**, 110 (1986).
[12] J. Massies and N. Grandjean, Phys. Rev. Lett. **71**, 1411 (1993).
[13] J. Eymery, S. Tatarenko, N. Bouchet, and K. Saminadayar, Appl. Phys. Lett. **64**, 3831 (1994).
[14] J. Fassbender, U. May, B. Schirmer, R. M. Jungblut, B. Hillebrands, and G. Guntherodt, Phys. Rev. Lett. **75**, 4476 (1995).
[15] U. May, J. Fassbender, and G. Guntherodt, Surf. Sci. **377/379**, 992 (1997).
[16] S. Andrieu, M. Finazzi, P. Bauer, H. Fischer, P. Lefevre, A. Traverse, K. Hricovini, G. Krill, and M. Piecuch, Phys. Rev. B **57**, 1985 (1998).
[17] J. Hartmann, A. Arnoult, L. Carbonell, V. Etgens, and S. Tatarenko, Appl. Surf. Sci. **123-124**, 283 (1998).
[18] G. Mula, C. Adelmann, S. Moehl, J. Oullier, and B. Daudin, Phys. Rev. B **64**, 195406 (2001).
[19] F. Dulot, P. Turban, B. Kierren, J. Eugene, M. Alnot, and S. Andrieu, Surf. Sci. **473**, 172 (2001).
[20] A. Bourret, C. Adelmann, B. Daudin, J. L. Rouviere, G. Feuillet, and G. Mula, Phys. Rev. B **63**, 245307 (2001).
[21] T. Koida, M. Lippmaa, D. Komiyama, M. Kawasaki, and H. Koinuma, Appl. Surf. Sci. **185**, 226 (2002).
[22] A. Nefedov, T. Schmitte, K. Theis-Brohl, H. Zabel, M. Doi, E. Schuster, and W. Keune, J. Phys. Condens. Matter **14**, 12273 (2002).
[23] X. H. Wei, Y. R. Li, J. Zhu, Y. Zhang, Z. Liang, and W. Huang, J. Phys. D: Appl. Phys. **38**, 4222 (2005).
[24] G. Niu, G. Saint-Girons, B. Vilquin, G. Delhaye, J.-L. Maurice, C. Botella, Y. Robach, and G. Hollinger, App. Phys. Lett. **95**, 062902 (2009).
[25] G. Niu, J. Penuelas, L. Largeau, B. Vilquin, J. L. Maurice, C. Botella, G. Hollinger, and G. Saint-Girons, Phys. Rev. B **83**, 054105 (2011).
[26] L. Carbonell, S. Tatarenko, J. Cibert, J. Hartmann, G. Mula, V. Etgens, and A. Arnoult, Appl. Surf. Sci. **123-124**, 283 (1998).
[27] P. Turban, L. Hennet, and S. Andrieu, Surf. Sci. **446**, 241 (2000).
[28] R. Kern and P. Müller, Surf. Sci. **392**, 103 (1997).
[29] P. Müller, P. Turban, L. Lapena, and S. Andrieu, Surf. Sci. **488**, 52 (2001).
[30] P. Turban, P. Müller, L. Lapena, and S. Andrieu, Appl. Surf. Sci. **188**, 97 (2002).
[31] P. Turban, F. Dulot, B. Kierren, and S. Andrieu, Appl. Surf. Sci. **177**, 282 (2001).
[32] M. van Hove, W. Wienberg, and C. Chan, in *Springer Series in Surface Science*, Vol. 6 (Springer, Berlin, 1986), p. 200.
[33] J. M. Hammersley, Ann. NY Acad. Sci. **86**, 844 (1960).
[34] S. Clarke and D. D. Vvedensky, Phys. Rev. Lett. **58**, 2235 (1987).